

Supporting Information

Multifunctional Magneto-Fluorescent Nanocarriers for Dual Mode Imaging and Targeted Drug Delivery

Ashish Tiwari[‡], Ashutosh Singh[‡], Ayan Debnath[‡], Ankur Kaul[§], Neha Garg^{*‡}, Rashi Mathur^{*§}, Anup Singh^{*‡} and Jaspreet K. Randhawa^{*‡}

[‡]School of Engineering, Indian Institute of Technology Mandi, Mandi, Himachal Pradesh-175005, India

[□]School of Basic Sciences, Indian Institute of Technology Mandi, Mandi, Himachal Pradesh-175005, India

[□]Centre for Biomedical Engineering, Indian Institute of Technology Delhi, Hauz Khas, New Delhi-110016, India

[§]Institute of Nuclear Medicine & Allied Sciences, Defence Research and Development Organization, Brig SK Mazumdar Road, New Delhi-110054, India

*Corresponding author postal address

Dr. Jaspreet Kaur Randhawa

Assistant Professor

School of Engineering, Indian Institute of Technology Mandi

A1 building, Kamand campus, Mandi, Himachal Pradesh -175005, India.

Telephone No. +91 1905-267056

Email: jaspreet@iitmandi.ac.in

Table of content

Figure S1. HR-TEM image of shell region of MFCSNPs.

Figure S2. FESEM-EDS elemental mapping analysis of MFCSNPs.

Scheme S1. Synthesis of folic acid and chitosan (FA-CHI) conjugate.

Figure S3. ¹H NMR spectra of folic acid, chitosan and folic acid and chitosan (FA-CHI) conjugate.

Figure S4. Zeta potential of MFCSNPs and MFCSNPs-FA-CHI-5FU nanocarriers.

Figure S5. Hydrodynamic diameter distribution of MFCSNPs and MFCSNPs-FA-CHI-5FU nanocarriers.

Figure S6. Stability of MFCSNPs-FA-CHI-5FU nanocarriers in aqueous solution analyzed by DLS measurements.

Figure S7. Nitrogen adsorption and desorption analysis of MFCSNPs.

Figure S8. BJH pore size distribution of MFCSNPs.

Figure S9. Nitrogen adsorption and desorption analysis of MFCSNPs-FA-CHI-5FU nanocarriers.

Figure S10. BJH pore size distribution of MFCSNPs-FA-CHI-5FU nanocarriers.

Figure S11. UV-Vis absorption spectra of folic acid, chitosan, folic acid-chitosan (FA-CHI) conjugate, MFCSNPs and MFCSNPs-FA-CHI-5FU nanocarriers.

Figure S12. Thermogravimetric analysis (TGA) curve of folic acid, chitosan, folic acid-chitosan (FA-CHI) conjugate, MFCSNPs and MFCSNPs-FA-CHI-5FU nanocarriers.

Figure S13. Excitation based photoluminescence emission spectra of MFCSNPs.

Figure S14. Photographs of MFCSNPs-FA-CHI-5FU nanocarriers with and without magnet.

Figure S15. UV-Vis calibration curve attained with different concentration of 5-Fluorouracil.

Figure S16. Linear fitting of UV-Vis calibration curve obtained for different concentration of 5-Fluorouracil.

Figure S17. Percentage of hemolysis persuaded by MFCSNPs and MFCSNPs-FA-CHI-5FU nanocarriers. Phosphate buffer solution (PBS) and 1% sodium dodecyl sulphate (SDS) were used as negative and positive control respectively.

Material Characterization

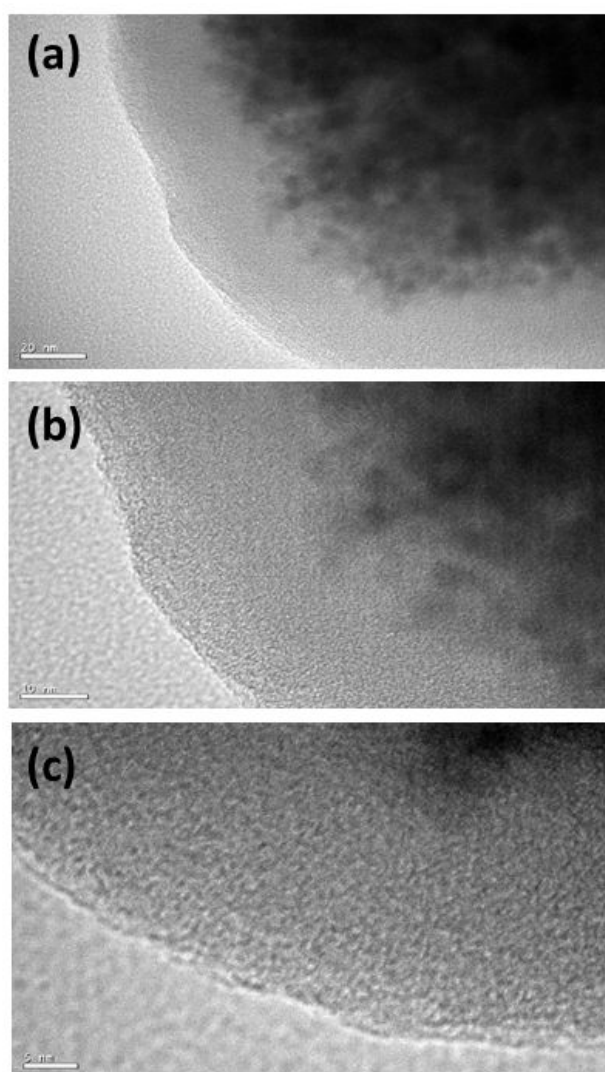


Figure S1. HR-TEM image of carbon shell present in MFCSNPs, no crystalline ordering was observed in the shell region. (Scale bar- (a) 20 nm, (b) 10 nm and (c) 5 nm respectively)

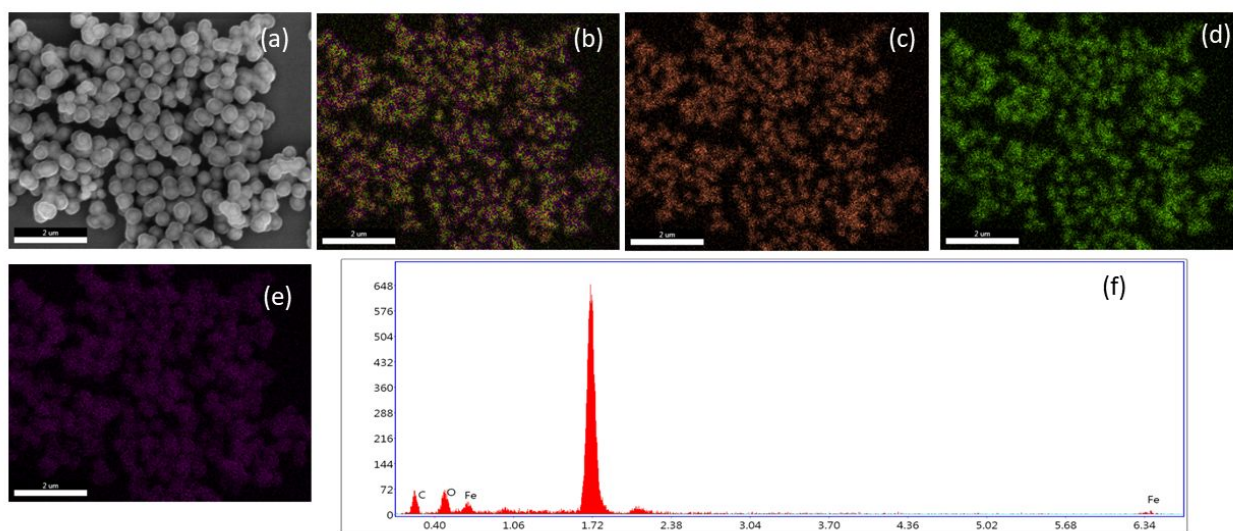
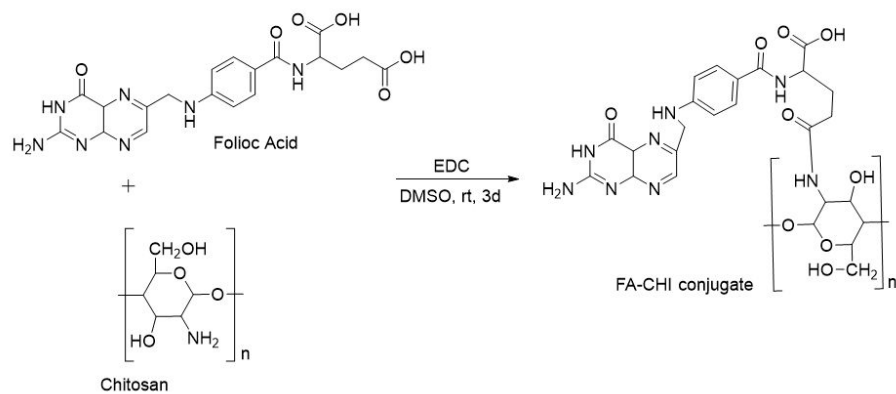


Figure S2. (a) FESEM images of MFCSNPs. (b) overlay image of elemental mapping with (c) iron, (d) oxygen and (e) carbon. (f) EDS spectra of MFCSNPs respectively. (Scale Bar-2 μm)

Scheme S1. Schematic diagram for the formation of folic acid and chitosan (FA-CHI) conjugate.



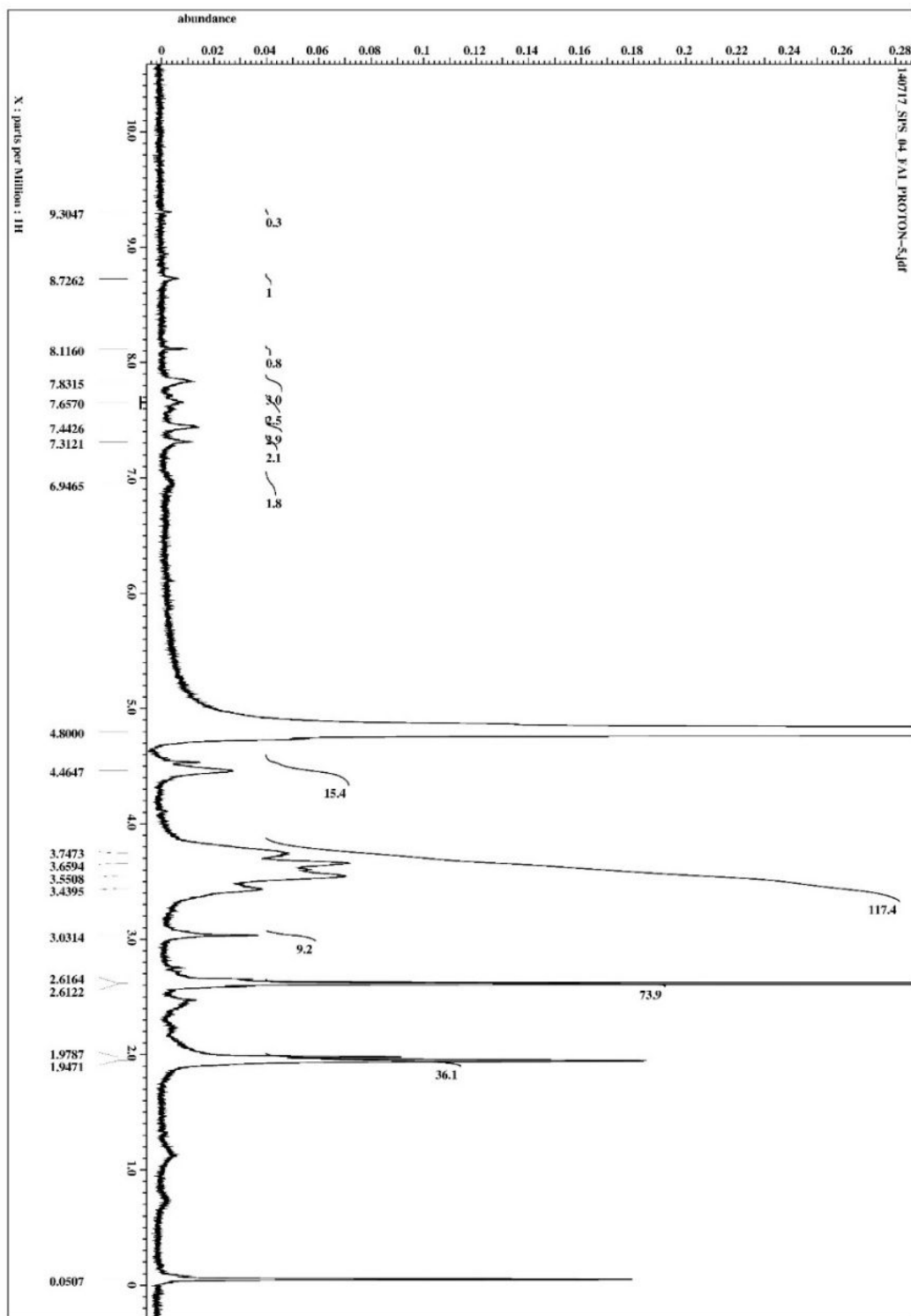


Figure S3 (a). ^1H NMR spectra of FA-CHI conjugates obtained in D_2O with 3% CD_3COOD solution.

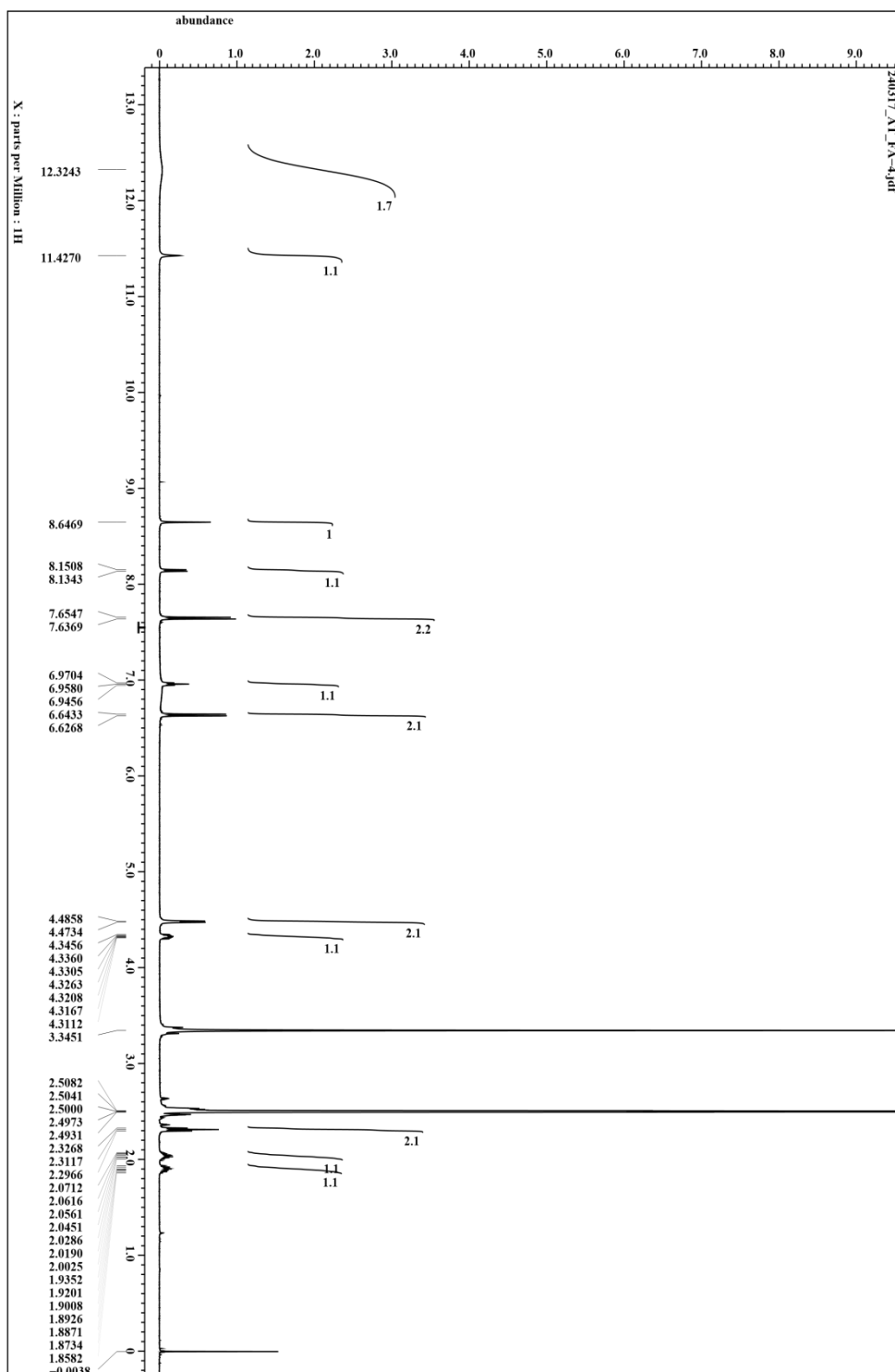


Figure S3 (b). ^1H NMR spectra of folic acid obtained in D_2O with 3% CD_3COOD solution.

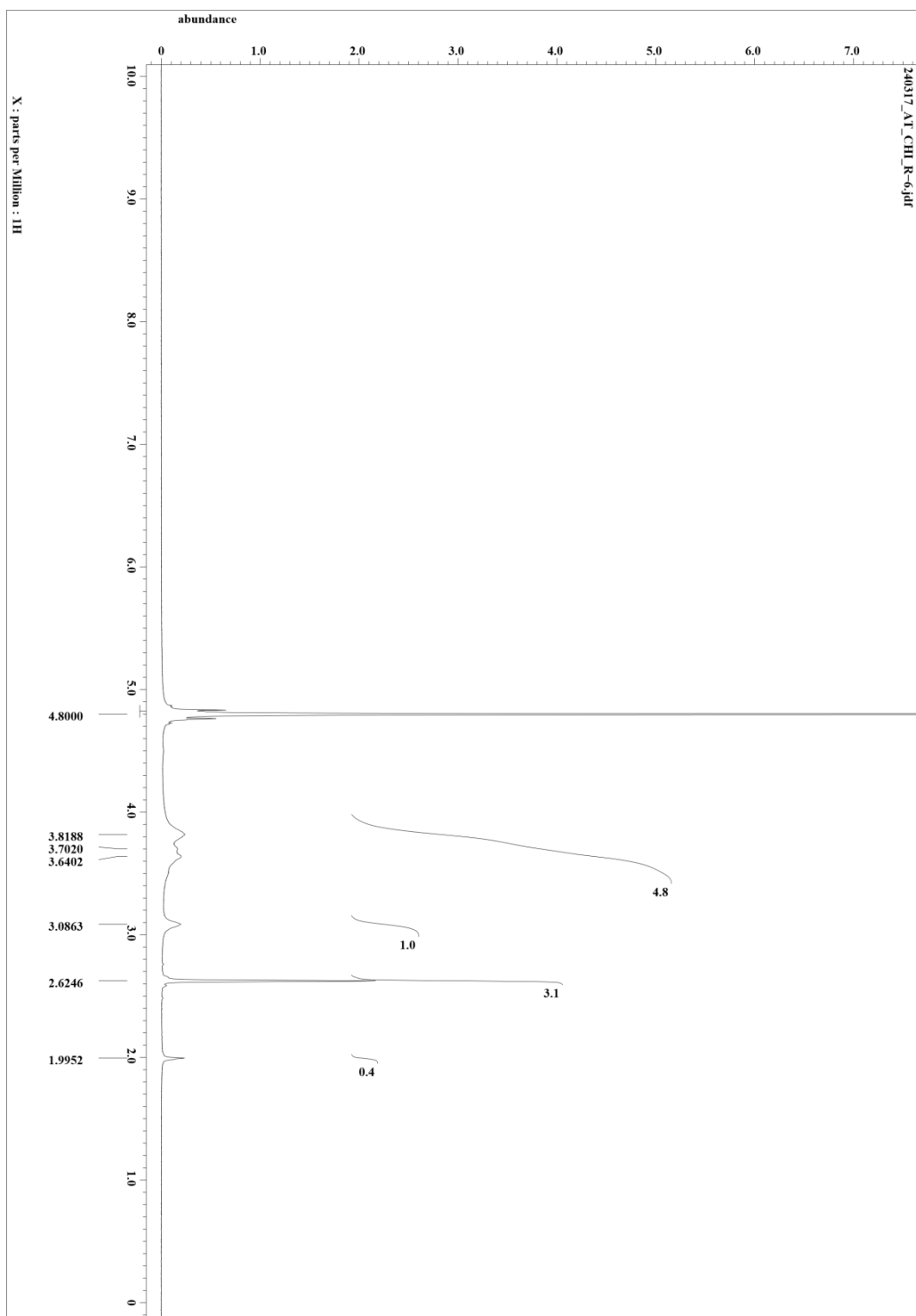


Figure S3 (c). ^1H NMR spectra of chitosan obtained in D_2O with 3% CD_3COOD solution.

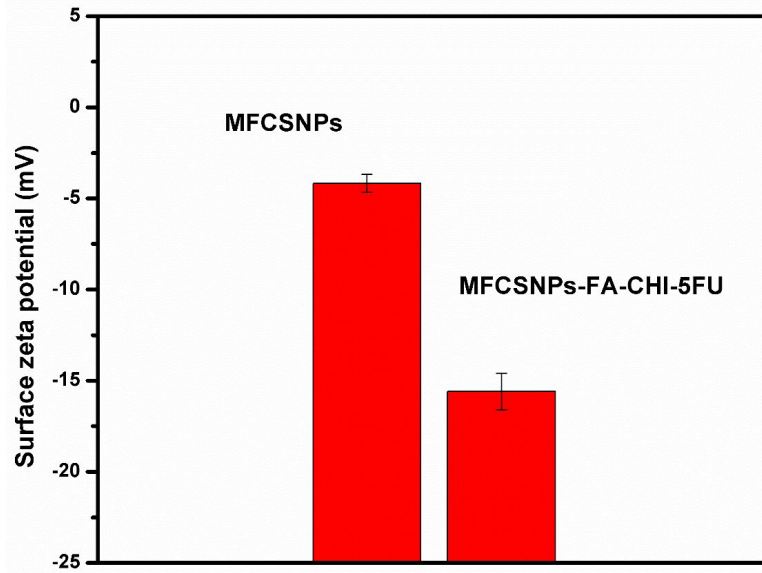


Figure S4. Zeta potential of MFCSNPs and MFCSNPs-FA-CHI-5FU nanocarriers.

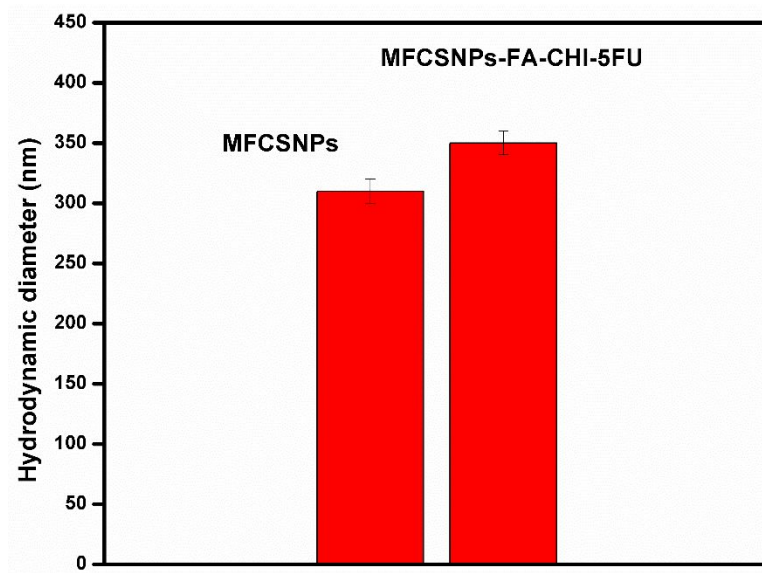


Figure S5. Hydrodynamic diameter distribution of MFCSNPs and MFCSNPs-FA-CHI-5FU nanocarriers.

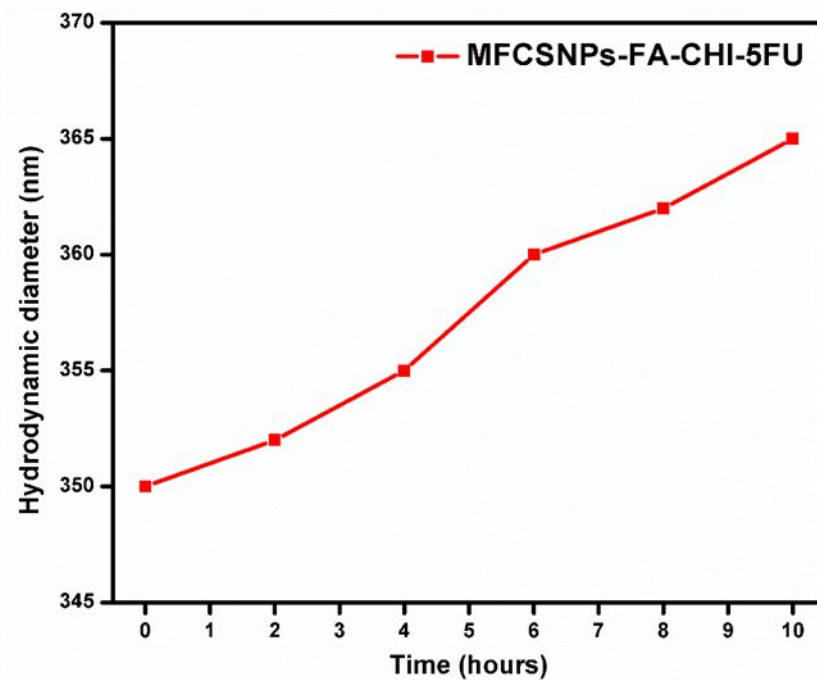


Figure S6. Stability of MFCSNPs-FA-CHI-5FU nanocarriers in aqueous solution analyzed by DLS measurements.

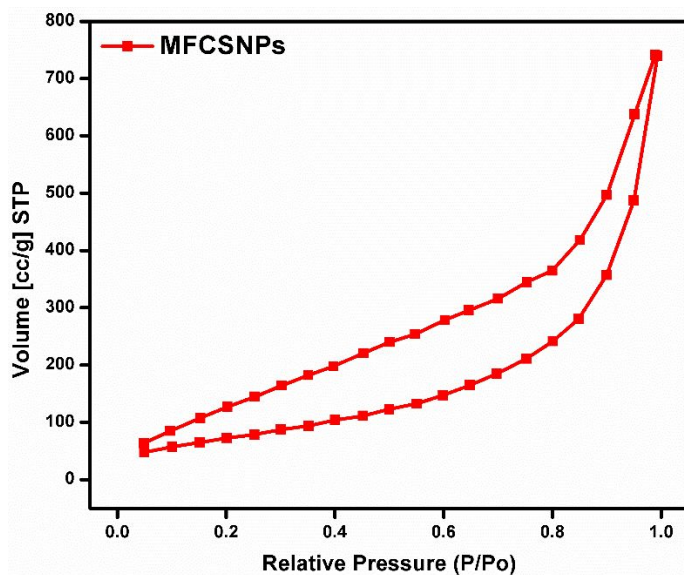


Figure S7. Nitrogen adsorption and desorption isotherms of MFCSNPs.

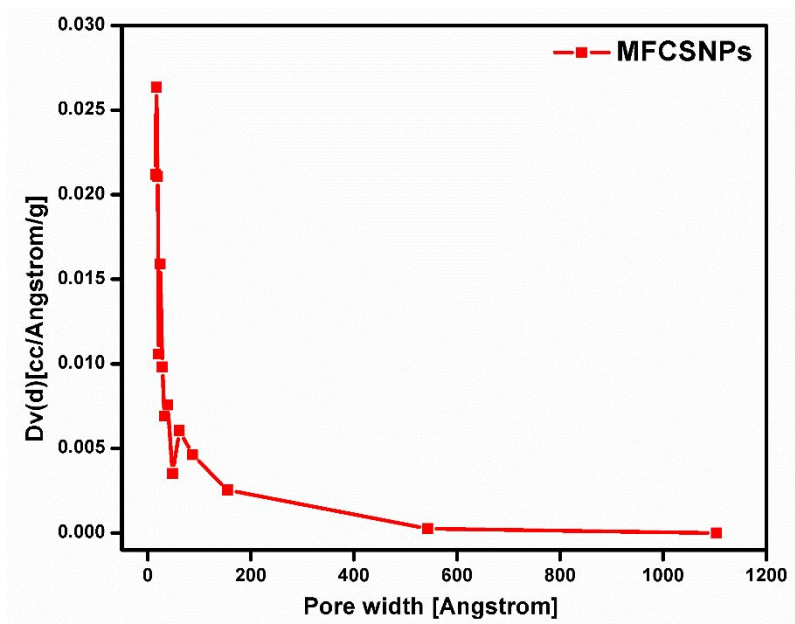


Figure S8. BJH pore size distribution of MFCSNPs.

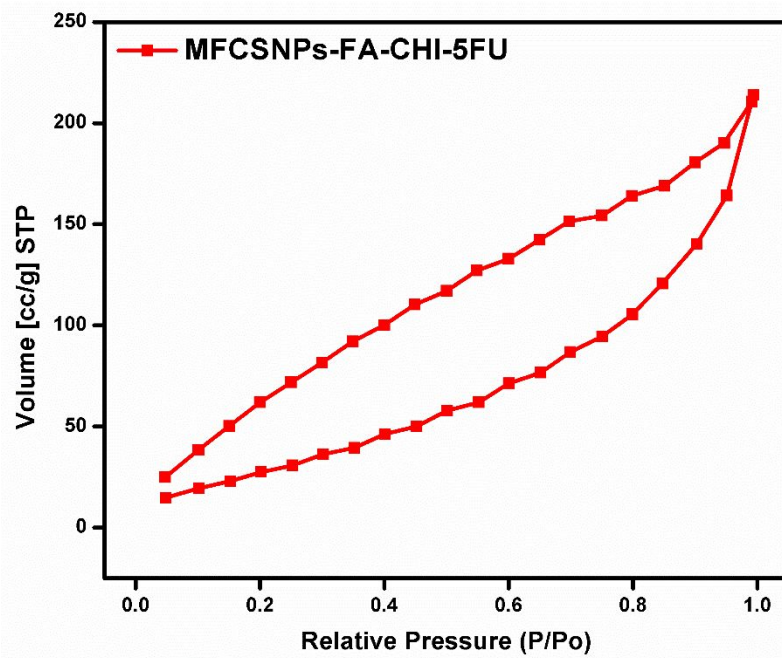


Figure S9. Nitrogen adsorption and desorption isotherms of MFCSNPs-FA-CHI-5FU nanocarriers.

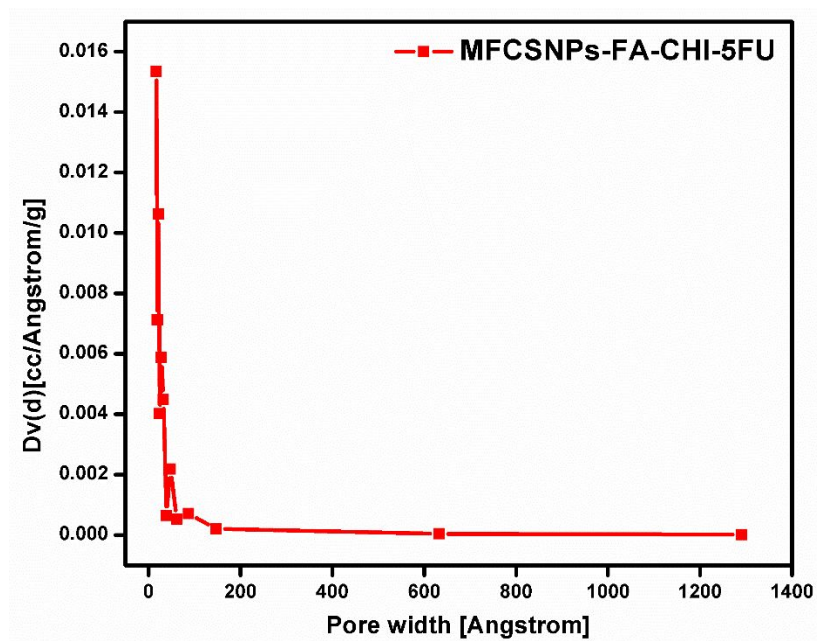


Figure S10. BJH pore size distribution of MFCSNPs-FA-CHI-5FU nanocarriers.

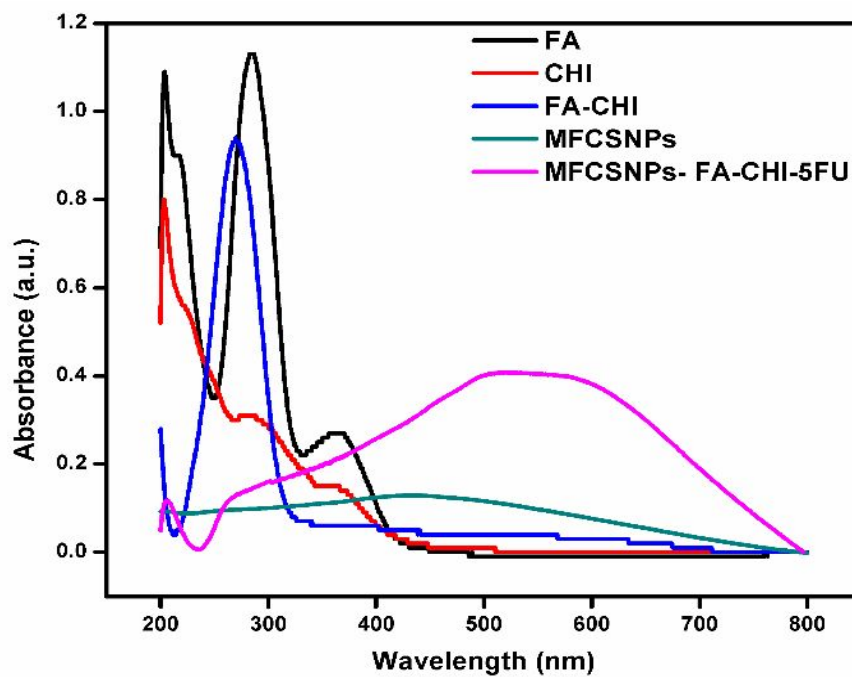


Figure S11. UV-Vis absorption spectra of folic acid, chitosan, folic acid-chitosan (FA-CHI) conjugate, MFCSNPs and MFCSNPs-FA-CHI-5FU nanocarriers respectively.

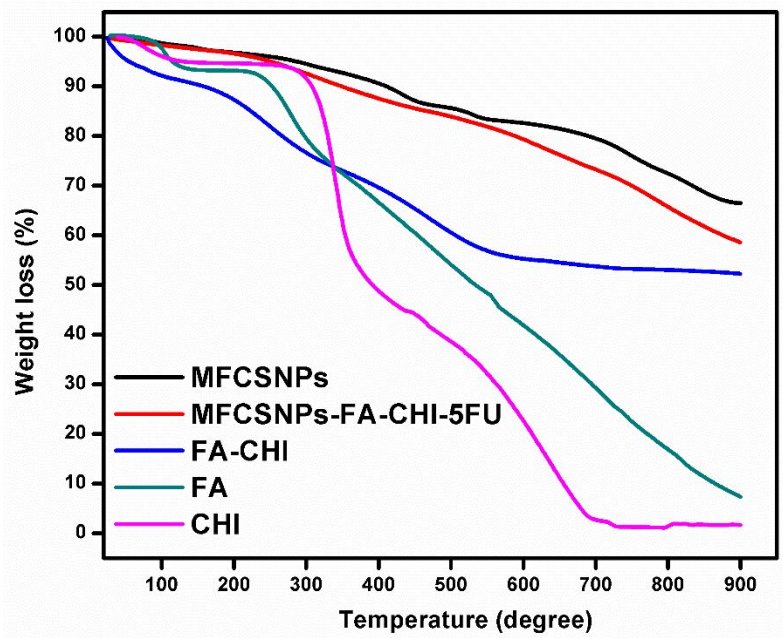


Figure S12. Thermogravimetric analysis (TGA) curve of folic acid, chitosan, folic acid-chitosan (FA-CHI) conjugate, MFCSNPs and MFCSNPs-FA-CHI-5FU nanocarriers respectively.

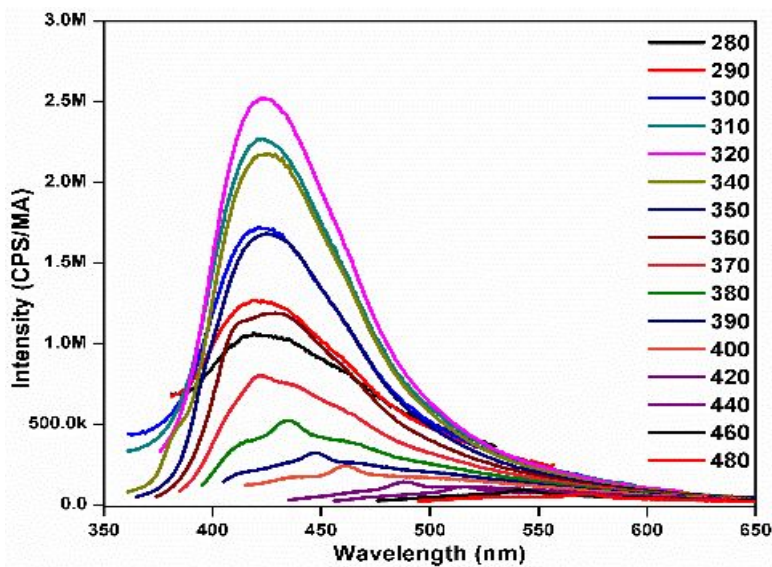


Figure S13. Excitation based photoluminescence emission spectra of MFCSNPs.

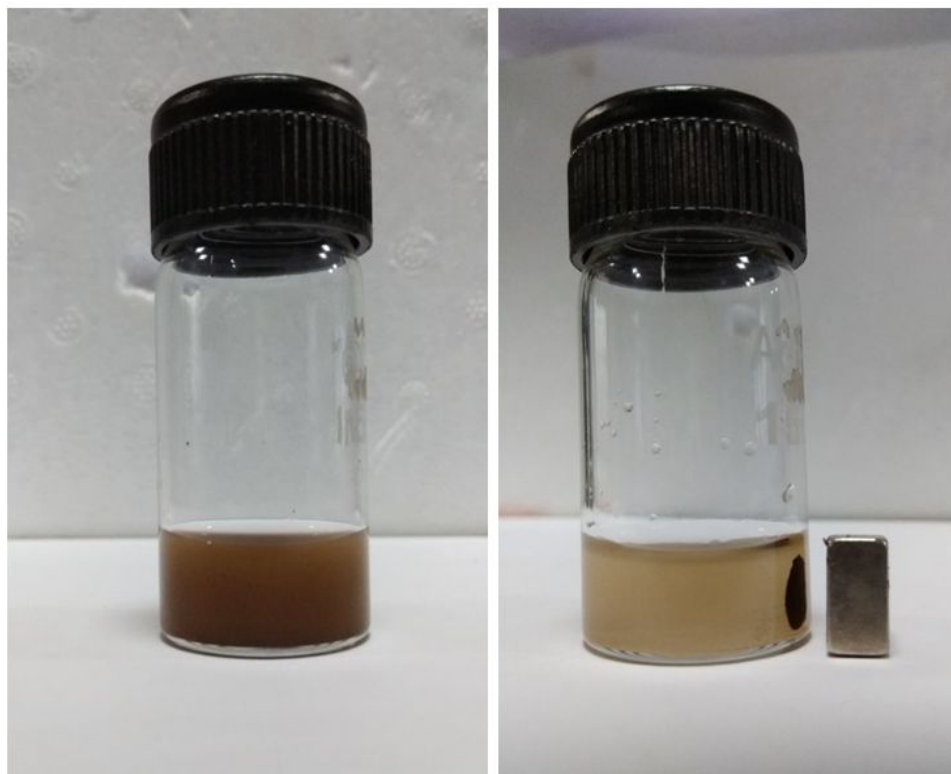


Figure S14. (a) Photograph of MFCSNPs dispersed in aqueous solution. (b) MFCSNPs after magnetic separation.

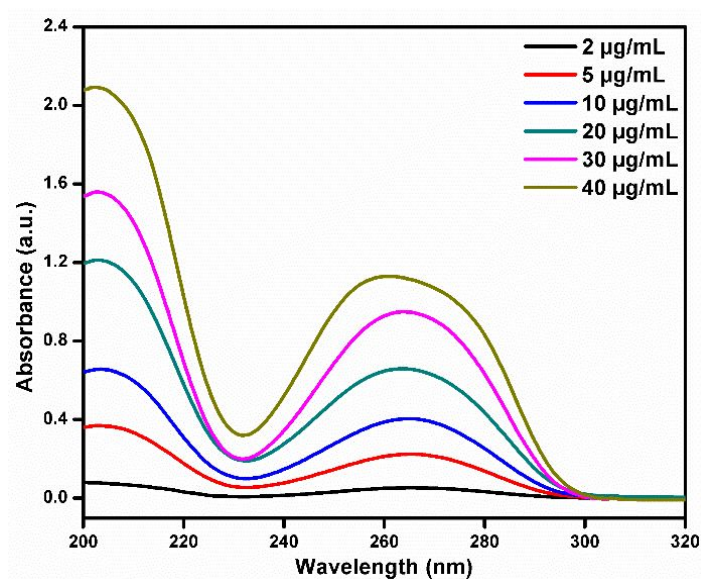


Figure S15. UV-Vis calibration curve attained with different concentration of 5-Fluorouracil in aqueous solution ranging from 2 to 40 µg/mL.

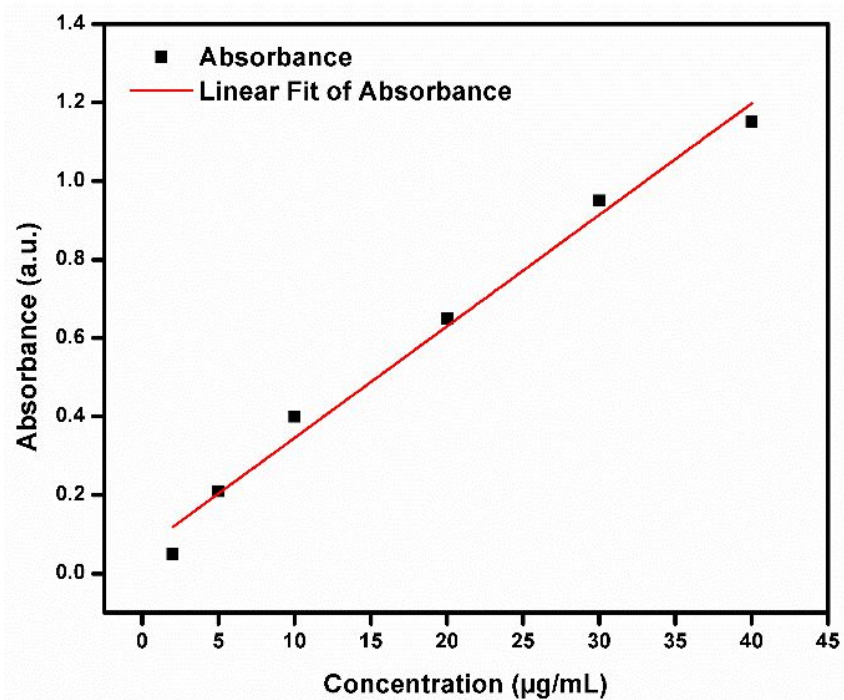


Figure S16. Linear fitting of UV-Vis calibration curve obtained for different concentration of 5-Fluorouracil in aqueous solution ranging from 2 to 40 µg/mL.

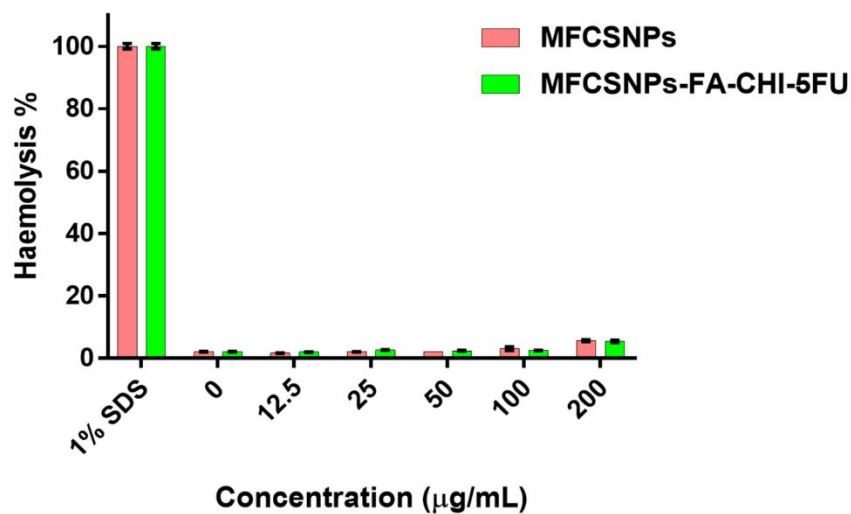


Figure S17. Percentage of hemolysis persuaded by MFCSNPs and MFCSNPs-FA-CHI-5FU nanocarriers. Phosphate buffer solution (PBS) and 1% sodium dodecyl sulphate (SDS) were used as negative and positive control respectively.